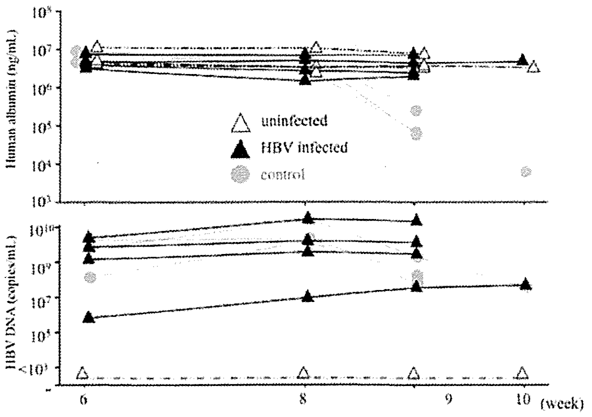

Fig. 3. Time course of mice transplanted with human PBMCs with DC depletion by clodronate 1 day before transplantation. Mice were treated with IP administration of clodronate 1 day before human PBMC transplantation. Time courses of human albumin concentration (upper panel) and HBV DNA titer (lower panel) in mouse serum are shown. Open and closed triangles correspond to 3 uninfected and 4 HBV-infected mice, respectively. Time courses of 3 mice infected with HBV and transplanted with human PBMC 3 days before transplantation (see Fig. 1C) are shown for comparison (shaded closed circle).

PBMC chimerism (Supporting Figs. 6A and 7A; Supporting Table 1). Activation of NK cells was not observed in this setting (Supporting Figs. 6B and 7B; Supporting Table 1). Depletion of DCs completely abolished the decline of both human albumin and HBV DNA (Fig. 3). Histological examination showed that hepatocyte degeneration was absent, and that there were no TUNEL-staining–positive cells (data not shown). Clodronate lyposomes may also nonspecifically deplete macrophages and monocytes in addition to DCs, but no monocytes or macrophages were observed when transplanted PBMCs were analyzed using Ficoll-Hypaque density gradient centrifugation, indicating that the clodronate administration was specifically associated with DC depletion in this study.

Analysis of Fas/FasL System in Massive HBV-Infected Hepatocyte Degeneration Model. We then assessed the importance of the Fas/FasL system and the occurrence of apoptosis in NK-cell–mediated human hepatocyte degeneration. Only HBV-infected human hepatocytes positive for HSA were positive for Fas antibody staining (Fig. 4A). TUNEL staining was also positive only in mice infected with HBV and inoculated with PBMCs (days 4 and 7). Measurement of mRNA levels in infected and uninfected livers showed that expression levels of Fas mRNA increased significantly upon HBV infection (Fig. 4B). To confirm that apoptosis of human hepatocytes was mediated by the Fas/FasL pathway and to determine whether IFN-α or IFN-γ played a role in the establishment of liver cell degeneration, we administered a blocking mAb against FasL, IFN-α, and IFN-γ 1 day before PBMC transplantation. Treatment of mice with antibody against FasL before PBMC completely abolished the decline of human albumin and HBV DNA (Fig. 5A). This abolishment of human albumin decline in mouse serum suggests that the Fas/FasL pathway almost exclusively eliminated infected hepatocytes in this model, which also suggests that Fas-mediated apoptosis could play an important role in FHB. Antibodies against IFN-α and IFN-γ inhibited IFN-induced ISG expression in mice livers (Supporting Fig. 8); however, these antibodies did not disturb the decline of HSA levels (Fig. 5A) and histological inflammation (Fig. 5B). Contact-dependent and -independent activation of NK cells by DCs has been reported previously.[23-25] Although IFN-α and IFN-γ play a role in their activation,[23,25,26] our results indicate that the effects of IFN-α are almost negligible in our experiments (Fig. 5A), suggesting that direct contact among these cells, or cytokines other than IFN-α and IFN-γ, are necessary to activate NK cells in this setting. NK cells have also been reported to exert antiviral effects by secreting IFN-γ. However, our results suggest that this mechanism does not work well in our model (Fig. 5A).

Discussion

In this study, we established a small animal model in which massive hepatocyte degeneration similar to FHB in humans is observed. Our initial attempts to detect human PBMCs in blood or any organ in transplanted mice failed even after injecting 2 × 10^7 cells, which is sufficient to establish human PBMC chimerism in SCID mice.[27] We assumed that failure to develop chimerism was the result of the activity of NK cells and macrophages because the activity of these cells in uPA-SCID mice is higher than in SCID mice.[28,29] Therefore, we attempted to eliminate these effects by administering clodronate and anti–asialo GM1 antibody, which are known to effectively eliminate these cells.[30,31] This assumption appears to be valid, because we were able to establish human PBMC chimerism and massive hepatocyte degeneration by suppressing these cells (Fig. 1).

HBV-specific CTLs have been reported to play an important role in eliminating the virus.[32-34] Accordingly, we attempted to detect HBV-specific CTLs in mice with massive hepatocyte degeneration. Unexpectedly, we failed to detect HBV-specific CTLs (Fig. 2A and Supporting Fig. 9) and instead found that infiltrating cells in the liver were CD3-negative NK cells

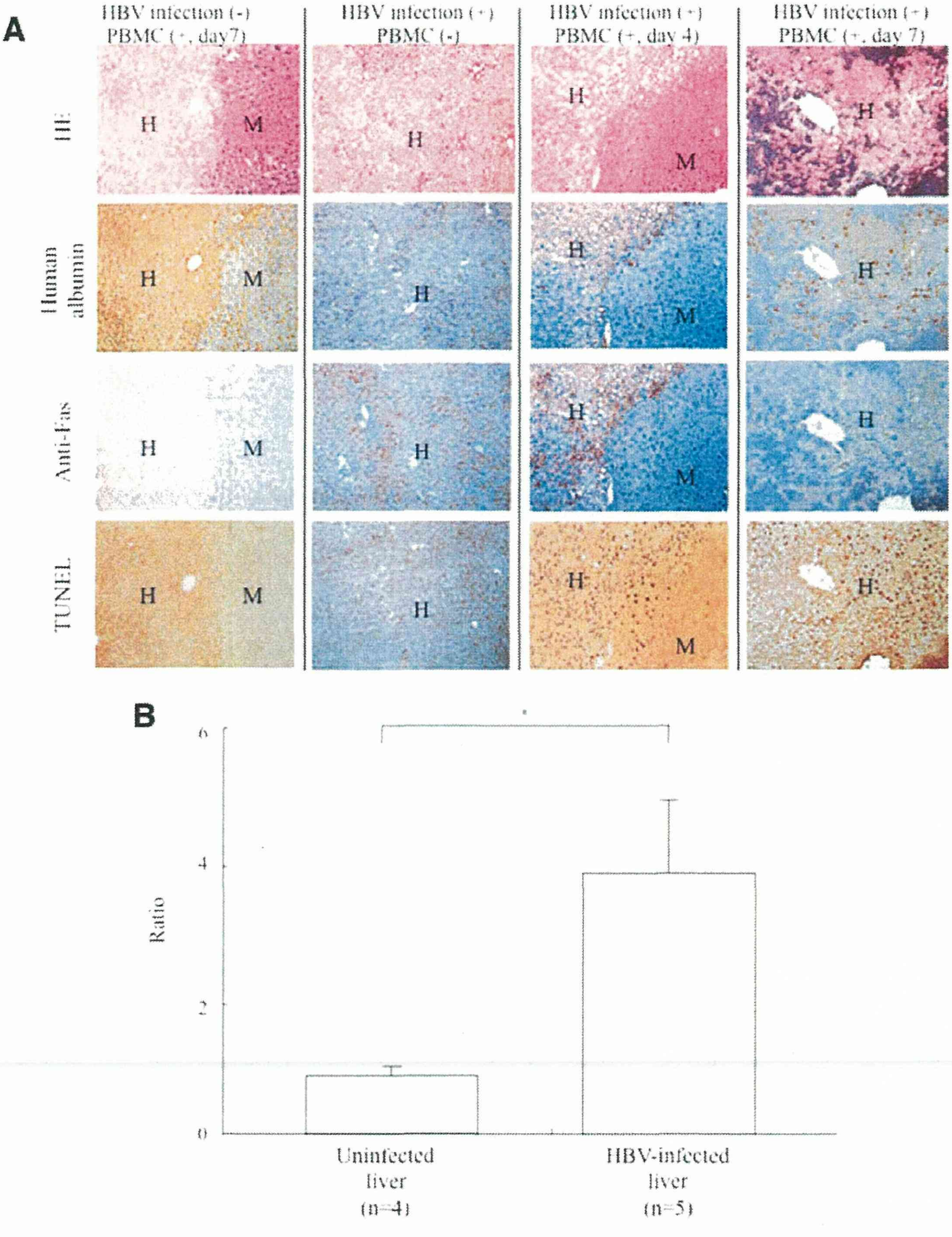

Fig. 4. Assessment of Fas expression in the liver in human hepatocyte chimeric mice. (A) Histological analysis of chimeric mice livers transplanted with human PBMCs but without HBV infection (day 7), with HBV infection but without PBMC transplantation, and with HBV infection and PBMC transplantation at days 4 and 7. Liver samples were stained with hematoxylin and eosin staining (HE), anti-human albumin antibody, anti-human Fas antibody, and TUNEL staining. Regions are shown as human (H) and mouse (M) hepatocytes, respectively (original magnification, 100×). Note that Fas antigen was expressed only in HBV-infected human hepatocytes, and TUNEL staining is only positive for HBV-infected and human PBMC-transplanted mice livers. Mouse hepatocytes were negative for all three stains. (B) Expression of Fas mRNA levels in uninfected and HBV-infected human hepatocytes. Data are represented as mean ± standard deviation. $^{*}P < 0.001$.

(Fig. 2B,D and Supporting Fig. 10). The reason for the absence of CTLs in our experiment is unknown, but this suggests that massive hepatocyte degeneration resembling fulminant hepatitis can be caused by NK cells as a main player, and recent reports demonstrating that NK cells contribute to severe acute and

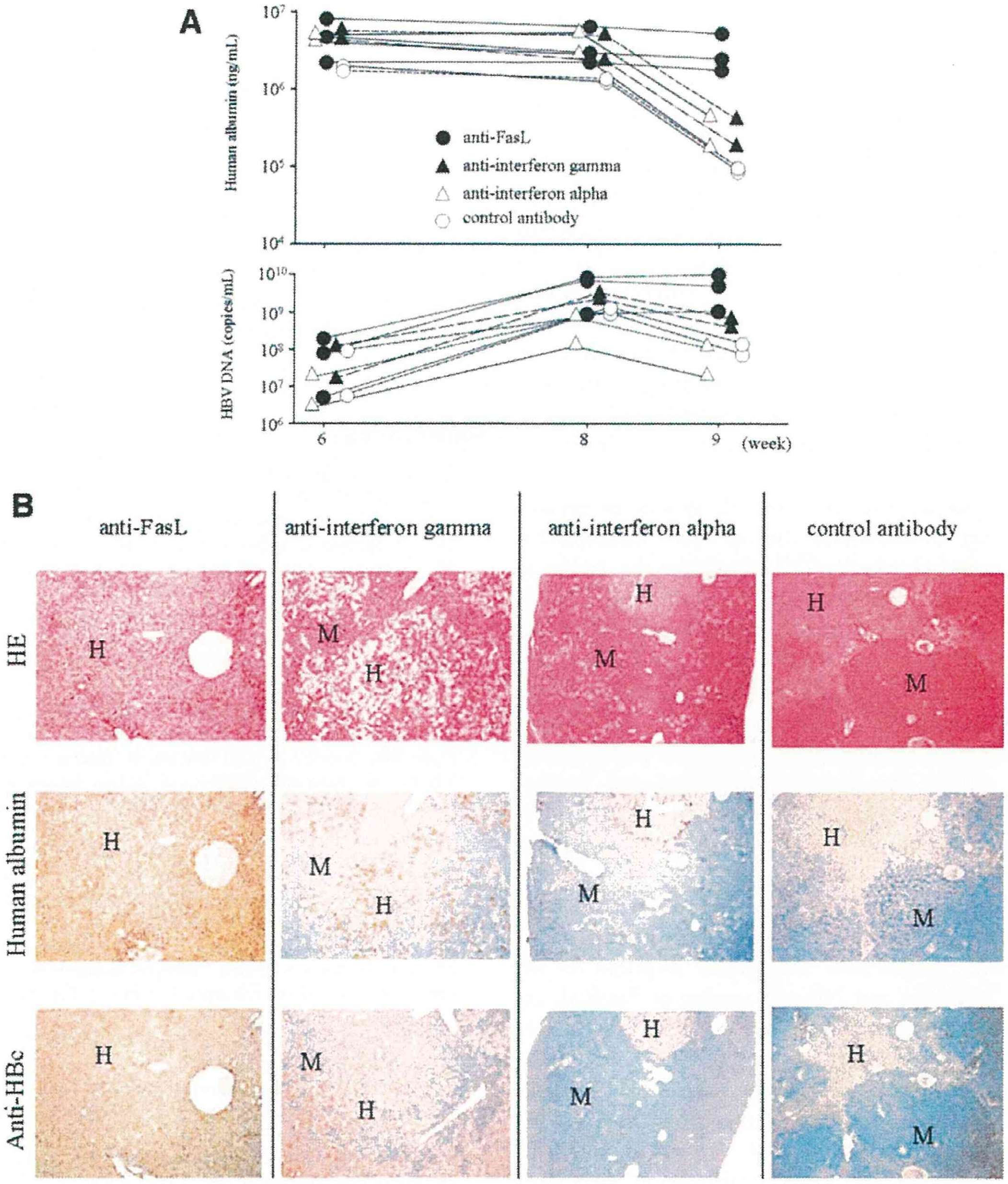

Fig. 5. Effect of anti-FasL, anti-IFN-γ and anti-IFN-α antibody administration on HSA and HBV DNA. (A) Time courses of HSA (upper panel) and HBV DNA (lower panel) before and 1 week after human PBMC transplantation are shown. Mice were pretreated with antibodies against human Fas-L, IFN-γ, and IFN-α before PBMC transplantation, as described in Materials and Methods. Isotype antibody was used as a control. (B) Histological analysis of livers of HBV-infected mice injected with anti-human FasL mAb, IFN-γ, IFN-α, and control antibody. Liver samples obtained from mice with human PBMCs at weeks 9 (day 7) were stained with hematoxylin and eosin staining (HE), antihuman albumin antibody, or antihepatitis B core antibody. Regions are shown as human (H) and mouse (M) hepatocytes, respectively (original magnification, 40×).

chronic hepatitis B (CHB) support this assertion.[11,35] We attempted to collect CTLs from HBV-infected patients and to establish hepatitis in chimeric mice. However, we rarely detected tetramer-positive CTLs in blood samples from chronically infected patients and were therefore unable to establish hepatitis using CD8-positive T cells. Consequently, a limitation of this study is that differential roles of NK cells and CTLs in massive liver cell death could not be examined.

Although it is not clear in this study how profoundly DC and NK cell activity plays a role in patients with FHB, our results suggest that the immune system can trigger severe hepatocyte degeneration. The importance of the activation of NK cells by DCs was evident, because depletion of DCs almost completely abolished the massive hepatocyte degeneration in this model (Supporting Fig. 10; Table 1). The interaction between NK cells and DCs is not well characterized, although it has been established that antigen-presenting accessory cells provide both indirect (i.e., soluble) and direct (i.e., contact-dependent) signals to T cells. Experiments in which NK cells are separated from pathogens and antigen-presenting cells by semipermeable membranes are cultured with supernatants from pathogen-activated DCs or in which cytokines are neutralized with blocking antibodies. These reports indicate that both soluble and contact-dependent signals may contribute to the activation of NK cells.[23,25,26]

The importance of the Fas/FasL system in hepatocyte damage in acute and chronic HBV infection has been reported previously.[37,38] However, the extent to which this system plays a role in human hepatitis B, especially fulminant hepatitis, is unknown. As shown in this study (Fig. 5A), inhibition of the Fas/FasL system by anti-Fas antibody dramatically reduced the effect of human PBMC transplantation. This showed the possibility that the Fas/FasL system plays an important role in the degeneration of infected hepatocytes in FHB. Further studies should be conducted to evaluate what immunological responses play important roles in human hepatitis B.

The importance of NK-cell activity suggests that the suppression of DCs and NK-cell activity or the Fas/FasL system might have therapeutic implications for FHB.[11,35] If DCs and NK-cell activity or Fas/FasL activity could be controlled in the early stages of severe acute or fulminant hepatitis, we might be able to control hepatitis activity and prevent subsequent liver failure. Of course, it would be necessary to monitor the development of chronic hepatitis after such treatment because DCs and NK cells contribute to early host defenses and shape subsequent adaptive immune response through complex cross-talk regulating the early phase of the immune response.[19,24,39,40]

We analyzed liver damage using HBV genotype C–infected mice in this study. However, HBV genotype C is associated with more severe histological liver damage than genotype B,[41] and future studies should compare immunological differences between genotypes B and C.

In summary, we established an animal model of FHB using highly repopulated human hepatocyte chimeric mice and transplanted human PBMCs. Modifications of this model will facilitate further research into acute and CHB using human immune cells, including HBV-directed CTL clones, suppressor and regulatory T cells, as well as immunological experiments to study interactions between DCs and NK cells. Such models may be useful to develop and evaluate new therapeutic strategies against HBV infection.

Acknowledgment: The authors thank Rie Akiyama and Yoko Matsumoto for their expert technical assistance. This work was carried out at the Analysis Center of Life Science, Natural Science Center for Basic Research and Development, Hiroshima University.

References

1. Bernal W, Auzinger G, Dhawan A, Wendon J. Acute liver failure. Lancet 2010;376:190-201.
2. Leifeld L, Cheng S, Ramakers J, Dumoulin FL, Trautwein C, Sauerbruch T, Spengler U. Imbalanced intrahepatic expression of interleukin 12, interferon gamma, and interleukin 10 in fulminant hepatitis B. HEPATOLOGY 2002;36:1001-1008.
3. Ozasa A, Tanaka Y, Orito E, Sugiyama M, Kang JH, Hige S, et al. Influence of genotypes and precore mutations on fulminant or chronic outcome of acute hepatitis B virus infection. Hepatology 2006;44:326-334.
4. Kawai T, Akira S. Toll-like receptor and RIG-I-like receptor signaling. Ann N Y Acad Sci 2008;1143:1-20.
5. Maini MK, Boni C, Lee CK, Larrubia JR, Reignat S, Ogg GS, et al. The role of virus-specific CD8(+) cells in liver damage and viral control during persistent hepatitis B virus infection. J Exp Med 2000;191:1269-1280.
6. Guidotti LG, Ando K, Hobbs MV, Ishikawa T, Runkel L, Schreiber RD, Chisari FV. Cytotoxic T lymphocytes inhibit hepatitis B virus gene expression by a noncytolytic mechanism in transgenic mice. Proc Natl Acad Sci U S A 1994;91:3764-3768.
7. Ando K, Moriyama T, Guidotti LG, Wirth S, Schreiber RD, Schlicht HJ, et al. Mechanisms of class I restricted immunopathology. A transgenic mouse model of fulminant hepatitis. J Exp Med 1993;178:1541-1554.
8. Cote PJ, Toshkov I, Bellezza C, Ascenzi M, Roneker C, Ann Graham L, et al. Temporal pathogenesis of experimental neonatal woodchuck hepatitis virus infection: increased initial viral load and decreased severity of acute hepatitis during the development of chronic viral infection. Hepatology 2000;32:807-817.
9. Chisari FV. Rous-Whipple Award Lecture. Viruses, immunity, and cancer: lessons from hepatitis B. Am J Pathol 2000;156:1117-1132.
10. Dunn C, Brunetto M, Reynolds G, Christophides T, Kennedy PT, Lampertico P, et al. Cytokines induced during chronic hepatitis B virus infection promote a pathway for NK cell-mediated liver damage. J Exp Med 2007;204:667-680.
11. Zhang Z, Zhang S, Zou Z, Shi J, Zhao J, Fan R, et al. Hypercytolytic activity of hepatic natural killer cells correlates with liver injury in chronic hepatitis B patients. Hepatology 2011;53:73-85.
12. Dandri M, Burda MR, Torok E, Pollok JM, Iwanska A, Sommer G, et al. Repopulation of mouse liver with human hepatocytes and *in vivo* infection with hepatitis B virus. Hepatology 2001;33:981-988.
13. Petersen J, Burda MR, Dandri M, Rogler CE. Transplantation of human hepatocytes in immunodeficient UPA mice: a model for the study of hepatitis B virus. Methods Mol Med 2004;96:253-260.
14. Ogata N, Miller RH, Ishak KG, Purcell RH. The complete nucleotide sequence of a pre-core mutant of hepatitis B virus implicated in fulminant hepatitis and its biological characterization in chimpanzees. Virology 1993;194:263-276.

15. Tateno C, Yoshizane Y, Saito N, Kataoka M, Utoh R, Yamasaki C, et al. Near completely humanized liver in mice shows human-type metabolic responses to drugs. Am J Pathol 2004;165:901-912.
16. Tsuge M, Hiraga N, Takaishi H, Noguchi C, Oga H, Imamura M, et al. Infection of human hepatocyte chimeric mouse with genetically engineered hepatitis B virus. HEPATOLOGY 2005;42:1046-1054.
17. Tsuge M, Hiraga N, Akiyama R, Tanaka S, Matsushita M, Mitsui F, et al. HBx protein is indispensable for development of viraemia in human hepatocyte chimeric mice. J Gen Virol 2010;91:1854-1864.
18. Kuhober A, Pudollek HP, Reifenberg K, Chisari FV, Schlicht HJ, Reimann J, Schirmbeck R. DNA immunization induces antibody and cytotoxic T cell responses to hepatitis B core antigen in H-2b mice. J Immunol 1996;156:3687-3695.
19. Banchereau J, Steinman RM. Dendritic cells and the control of immunity. Nature 1998;392:245-252.
20. Shortman K, Liu YJ. Mouse and human dendritic cell subtypes. Nat Rev Immunol 2002;2:151-161.
21. Sandhu J, Shpitz B, Gallinger S, Hozumi N. Human primary immune response in SCID mice engrafted with human peripheral blood lymphocytes. J Immunol 1994;152:3806-3813.
22. Gonzalez SF, Lukacs-Kornek V, Kuligowski MP, Pitcher LA, Degn SE, Kim YA, et al. Capture of influenza by medullary dendritic cells via SIGN-R1 is essential for humoral immunity in draining lymph nodes. Nat Immunol 2010;11:427-434.
23. Fernandez NC, Lozier A, Flament C, Ricciardi-Castagnoli P, Bellet D, Suter M, et al. Dendritic cells directly trigger NK cell functions: cross-talk relevant in innate anti-tumor immune responses *in vivo*. Nat Med 1999;5:405-411.
24. Ferlazzo G, Tsang ML, Moretta L, Melioli G, Steinman RM, Munz C. Human dendritic cells activate resting natural killer (NK) cells and are recognized via the NKp30 receptor by activated NK cells. J Exp Med 2002;195:343-351.
25. Andoniou CE, van Dommelen SL, Voigt V, Andrews DM, Brizard G, Asselin-Paturel C, et al. Interaction between conventional dendritic cells and natural killer cells is integral to the activation of effective antiviral immunity. Nat Immunol 2005;6:1011-1019.
26. Walzer T, Dalod M, Robbins SH, Zitvogel L, Vivier E. Natural-killer cells and dendritic cells: "l'union fait la force". Blood 2005;106:2252-2258.
27. Mosier DE, Gulizia RJ, Baird SM, Wilson DB, Spector DH, Spector SA. Human immunodeficiency virus infection of human-PBL-SCID mice. Science 1991;251:791-794.
28. Kawahara T, Douglas DN, Lewis J, Lund G, Addison W, Tyrrell DL, et al. Critical role of natural killer cells in the rejection of human hepatocytes after xenotransplantation into immunodeficient mice. Transpl Int 2010;23:934-943.
29. Morosan S, Hez-Deroubaix S, Lunel F, Renia L, Giannini C, Van Rooijen N, et al. Liver-stage development of *Plasmodium falciparum*, in a humanized mouse model. J Infect Dis 2006;193:996-1004.
30. Dorshkind K, Pollack SB, Bosma MJ, Phillips RA. Natural killer (NK) cells are present in mice with severe combined immunodeficiency (SCID). J Immunol 1985;134:3798-3801.
31. Ito M, Hiramatsu H, Kobayashi K, Suzue K, Kawahata M, Hioki K, et al. NOD/SCID/gamma(c)(null) mouse: an excellent recipient mouse model for engraftment of human cells. Blood 2002;100:3175-3182.
32. Thimme R, Wieland S, Steiger C, Ghrayeb J, Reimann KA, Purcell RH, Chisari FV. CD8(+) T cells mediate viral clearance and disease pathogenesis during acute hepatitis B virus infection. J Virol 2003;77:68-76.
33. Rehermann B, Fowler P, Sidney J, Person J, Redeker A, Brown M, et al. The cytotoxic T lymphocyte response to multiple hepatitis B virus polymerase epitopes during and after acute viral hepatitis. J Exp Med 1995;181:1047-1058.
34. Webster GJ, Reignat S, Maini MK, Whalley SA, Ogg GS, King A, et al. Incubation phase of acute hepatitis B in man: dynamic of cellular immune mechanisms. HEPATOLOGY 2000;32:1117-1124.
35. Zou Y, Chen T, Han M, Wang H, Yan W, Song G, et al. Increased killing of liver NK cells by Fas/Fas ligand and NKG2D/NKG2D ligand contributes to hepatocyte necrosis in virus-induced liver failure. J Immunol 2010;184:466-475.
36. Newman KC, Riley EM. Whatever turns you on: accessory-cell-dependent activation of NK cells by pathogens. Nat Rev Immunol 2007;7:279-291.
37. Galle PR, Hofmann WJ, Walczak H, Schaller H, Otto G, Stremmel W, et al. Involvement of the CD95 (APO-1/Fas) receptor and ligand in liver damage. J Exp Med 1995;182:1223-1230.
38. Rivero M, Crespo J, Fábrega E, Casafont F, Mayorga M, Gomez-Fleitas M, Pons-Romero F. Apoptosis mediated by the Fas system in the fulminant hepatitis by hepatitis B virus. J Viral Hepat 2002;9:107-113.
39. Moretta A. Natural killer cells and dendritic cells: rendezvous in abused tissues. Nat Rev Immunol 2002;2:957-964.
40. Asselin-Paturel C, Trinchieri G. Production of type I interferons: plasmacytoid dendritic cells and beyond. J Exp Med 2005;202:461-465.
41. Orito E, Ichida T, Sakugawa H, Sata M, Horiike N, Hino K, et al. Geographic distribution of hepatitis B virus (HBV) genotype in patients with chronic HBV infection in Japan. HEPATOLOGY 2001;34:590-594.

ORIGINAL ARTICLE

MicroRNA-221/222 upregulation indicates the activation of stellate cells and the progression of liver fibrosis

Tomohiro Ogawa,[1,2,3] Masaru Enomoto,[1] Hideki Fujii,[1] Yumiko Sekiya,[1,2]
Katsutoshi Yoshizato,[2,4] Kazuo Ikeda,[5] Norifumi Kawada[1,2]

[1]Department of Hepatology, Graduate School of Medicine, Osaka City University, Osaka, Japan
[2]Liver Research Center, Graduate School of Medicine, Osaka City University, Osaka, Japan
[3]Center for the Advancement of Higher Education, Faculty of Engineering, Kinki University, Hiroshima, Japan
[4]PhoenixBio Co Ltd., Hiroshima, Japan
[5]Department of Anatomy and Cell Biology, Graduate School of Medicine, Nagoya City University, Aichi, Japan

Correspondence to
Professor Norifumi Kawada, Department of Hepatology, Graduate School of Medicine, Osaka City University, 1-4-3, Asahimachi, Abeno, Osaka 545-8585, Japan; kawadanori@med.osaka-cu.ac.jp

Revised 1 December 2011
Accepted 15 December 2011

Published Online First
20 January 2012

ABSTRACT

Background MicroRNAs (miRNAs) are important in hepatic pathophysiology and the development of liver cancer.

Objective To explore miRNAs that are regulated with the progression of liver fibrosis caused by chronic liver disease.

Design The regulated miRNAs in human livers infected with hepatitis C virus were identified by microarray analysis. Their expression in human livers with non-alcoholic steatohepatitis, mouse livers from two fibrosis models and cultured stellate cells was validated by real-time RT-PCR. The regulation of miR-222 expression in stellate cells by nuclear factor kappa B (NF-κB) was assayed. Finally, the effects of an miR-222 precursor or inhibitor on the expression of cyclin-dependent kinase inhibitor 1B (CDKN1B) and the growth of LX-2 cells were determined.

Results It was found that miR-199a-5p/199a-3p and miR-221/222 were upregulated in the human liver in a fibrosis progression—dependent manner. Among these miRNAs, miR-221/222 were upregulated in LX-2 cells and increased during the course of culture-dependent activation of mouse primary stellate cells, in a manner similar to the expression of α1(I) collagen and α-smooth muscle actin mRNAs. The expression of miR-221/222 increased in mouse models of liver fibrosis. In contrast, an NF-κB inhibitor significantly suppressed the miR-222 induction that was stimulated in culture by transforming growth factor α or tumour necrosis factor α. Although overexpression or downregulation of miR-222 failed to regulate the growth of LX-2 cells, miR-222 bound to the *CDKN1B* 3′UTR and regulated the expression of the corresponding protein.

Conclusion miR-221/222 may be new markers for stellate cell activation and liver fibrosis progression.

Significance of this study

What is already known about this subject?

- The abundance of miR-221/222 increases in human hepatocellular carcinoma (HCC).
- miR-221/222 elicit their oncogenic effects via the downregulation of tumour suppressors, such as p27, p57 and PTEN.
- The expression of miR-221/222 is induced by NF-κB activation in prostate carcinoma and glioblastoma cells.

What are the new findings?

- The expression of miR-221/222 increases with the progression of human liver fibrosis and is correlated with the expression levels of α1 (I) collagen and α-smooth muscle actin mRNAs.
- The expression of miR-221/222 is highly correlated with α1 (I) collagen mRNA expression in mouse stellate cells in culture.
- miR-222 expression is inhibited by an NF-κB inhibitor and upregulated by NF-κB activators, such as tumour necrosis factor α and transforming growth factor α.

How might they impact on clinical practice in the foreseeable future?

- miR-221/222 have the potential to be new markers for stellate cell activation and liver fibrosis progression in humans.
- The pattern of miR-221/222 expression can serve as a useful tool for understanding and investigating the mechanism of the progression of liver fibrosis.
- The miRNA profiling of human liver fibrosis contributes to the identification of predictors of disease prognosis and potential therapeutic targets.

INTRODUCTION

Hepatic fibrosis is a consequence of the accumulation of extracellular matrix (ECM) components in the liver. This process is caused by the persistent liver damage and wound healing reaction induced by chronic viral hepatitis, alcohol abuse, non-alcoholic steatohepatitis (NASH) and several other aetiologies and can progress to cirrhosis and hepatocellular carcinoma (HCC).[1] Hepatitis C virus (HCV) infection is one of the leading causes of end-stage liver diseases worldwide and the most common indication for liver transplantation in the USA and Europe. In addition, non-alcoholic fatty liver disease and its progressive form, NASH, have become urgent clinical problems owing to the increasing prevalence of metabolic syndrome.[2–4] Because fibrotic liver disease has thus become a global health problem, it is important to understand the molecular mechanisms of hepatic fibrosis, irrespective of the cause, to establish proper therapeutic strategies and to identify diagnostic markers of this disease.

It is generally accepted that excessive production of ECM components by activated hepatic stellate cells and myofibroblasts is responsible for hepatic fibrosis.[5 6] Hepatic stellate cells exist in Disse's space and store vitamin A under physiological conditions.[7] When liver injury occurs, these cells become activated in response to oxidative stress, growth factors and inflammatory stimuli that are produced by damaged hepatocytes, resident macrophages (Kupffer cells), infiltrating inflammatory cells and aggregated platelets. The hepatic stellate cells then undergo transformation into myofibroblast-like cells that express α-smooth muscle actin (αSMA).[5] Activated stellate cells deposit ECM components, including types I and III collagen, fibronectin and laminin, at the site of local tissue damage and secrete profibrogenic mediators, such as transforming growth factor β (TGFβ), connective tissue growth factor and platelet-derived growth factor, thereby playing a pivotal role in liver fibrogenesis.[6]

MicroRNAs (miRNAs) are small, endogenous, non-coding RNAs that interact with the 3′ untranslated region (UTR) of target mRNAs, resulting in the inhibition of translation or the promotion of mRNA degradation.[8 9] miRNAs are important in proliferation,[10] development[11] and differentiation[12] in many cell types and are involved in the development of many diseases, including cancer.[13–15] miR-122 has been the best studied miRNA with regard to liver pathophysiology. For example, miR-122 is highly abundant in the human liver and is essential for HCV replication.[16–19] Interferon β rapidly modulates the expression of miR-122, which has sequence-predicted targets within the HCV RNA.[20] In chronic hepatitis C, decreased miR-122 has been associated with an absence of virological response to interferon and ribavirin treatment.[21] miR-21, -34a, -93, -96, -221/222 and -519a increase and, in contrast, let-7c decreases in human HCC.[22] The expression levels of miR-21 and miR-122 correlate with the histological evaluation of HCV-induced liver disease.[23]

Here, we show that the expression of miR-221/222 increased with the progression of liver fibrosis and significantly correlated with the expression of α1 (I) collagen (Col1A1) and αSMA mRNAs in human fibrotic livers. The expression of miR-221/222 in human fibrotic livers was also reproduced in mouse models of hepatic fibrosis. Interestingly, miR-221/222 were more highly expressed in a human stellate cell line, LX-2, than in HCC cell lines and their expression was induced with the activation of mouse stellate cells. Finally, we show that the expression of miR-222 in stellate cells may be regulated by the activation of nuclear factor kappa B (NF-κB). Taken together, our findings indicate that miR-221/222 upregulation is a new marker for stellate cell activation and liver fibrosis progression that could be used for the clinical diagnosis of liver fibrosis.

MATERIALS AND METHODS

Materials

Precursors and inhibitors of miR-222 and the negative control miRNA were purchased from Ambion (Austin, Texas, USA). Dulbecco's modified Eagle's medium (DMEM) and fetal bovine serum (FBS) were purchased from Sigma Chemical Co (St Louis, Missouri, USA). The mouse monoclonal antibody against cyclin-dependent kinase inhibitor 1B (CDKN1B (p27, Kip1)) was from Cell Signaling Technology Inc (Beverly, Massachusetts, USA) and that against glyceraldehyde 3-phosphate dehydrogenase (GAPDH) was from Chemicon International Inc (Temecula, California, USA). Enhanced Chemiluminescence Plus detection reagent was from GE Healthcare (Buckinghamshire, UK). Immobilon P membranes were from Millipore Corp. (Bedford, Massachusetts, USA). Recombinant human TGFα and mouse tumour necrosis factor (TNF)α were from R&D Systems, Inc (Minneapolis, Minnesota, USA). 6-Amino-4-(4-phenoxyphenylethylamono)quinazoline (QNZ) was from EMD Chemicals, Inc (Gibbstown, New Jersey, USA). All other reagents were purchased from Sigma Chemical Co or Wako Pure Chemical Co (Osaka, Japan).

Liver biopsy specimens

Liver biopsy specimens were obtained from 35 patients with chronic hepatitis C genotype 1 infection and 26 patients with NASH using a 15-gauge Tru-Cut biopsy needle (Hakko Inc., Tokyo, Japan) under ultrasound guidance (table 1). Of the 26 patients with NASH, oral hypoglycaemic agents were given to four patients (sulphonylureas to three and metformin to one), antihypertensive agents to eight (angiotensin receptor blockers to five and calcium channel blockers to three) and anti-hyperlipidaemic agents to eight (statins to five and fibrates to three) at the time of liver biopsy. Informed consent was obtained from all patients before biopsy. All procedures were in accordance with the Helsinki Declaration of 1975 (2008 revision). Biopsied liver tissues were fixed in 10% formalin solution and then embedded in paraffin. The stage of liver fibrosis was evaluated according to the METAVIR scoring system in patients with chronic hepatitis C[24] and the Brunt classification in patients with NASH.[4] A portion of each biopsy sample was immediately placed in RNAlater (Qiagen, Valencia, California, USA), temporarily stored at −20°C and then used to extract total RNAs using the mirVana miRNA Isolation Kit (Applied

Table 1 Baseline characteristics of patients

Characteristics	All patients with CHC (n=35)	Patients with CHC undergoing microarray analysis (n=22)	Patients with NASH (n=26)
Age (years)*	59±9	58±6	58±12
Female sex (%)†	20 (57)	11 (50)	14 (54)
Interferon-naïve (%)†	24 (69)	15 (68)	
ALT (IU/l)‡	57 (34–99)	88 (51–171)	69 (28–226)
Albumin (g/dl)*	4.0±0.3	4.0±0.3	4.0±0.5
Platelet count ($\times 10^9$/l)*	179±53	169±46	184±54
HCV RNA ($\log_{10}$ copies/ml)*	6.1±1.0	6.0±1.2	
Grade of necroinflammation† (A0/A1/A2/A3)	3/23/8/1	2/13/6/1	0/10/10/6
Stage of fibrosis† (F1/F2/F3/F4)	19/7/7/2	11/4/5/2	7/8/8/3

*Mean±SD.
†Numbers of patients.
‡Median (IQR).
ALT, alanine aminotransferase; CHC, chronic hepatitis C; HCV, hepatitis C virus; NASH, non-alcoholic steatohepatitis.

Table 2 List of primer sequences

Gene		Sequence (5′-3′)	Accession No
Human	Forward	CCCGGGTTTCAGAGACAACTTC	NM_000088
Col1A1	Reverse	TCCACATGCTTTATTCCAGCAATC	
Human	Forward	GACAATGGCTCTGGGCTCTGTAA	NM_001613
αSMA	Reverse	CTGTGCTTCGTCACCCACGTA	
Human	Forward	AGCTTGCCCGAGTTCTACTACAG	NM_004064
CDKN1B	Reverse	ACCAAATGCGTGTCCTCAGAGT	
Human	Forward	CTCTACTGGCGAAACCTGTATCC	NM_000089
Col1A2	Reverse	TCTCCTAGCCAGACGTGTTTCTT	
Human	Forward	CTGGCCACAACTGCCAAATG	NM_001145938
MMP1	Reverse	CTGTCCCTGAACAGCCCAGTACTTA	
Human	Forward	TGACATCAAGGGCATTCAGGAG	NM_001127891
MMP2	Reverse	TCTGAGCGATGCCATCAAATACA	
Human	Forward	TCGAACTTTGACAGCGACAAGAA	NM_004994
MMP9	Reverse	TCAGTGAAGCGGTACATAGGGTACA	
Human	Forward	GGATACTTCCACAGGTCCCACAA	NM_003254
TIMP1	Reverse	CTGCAGGTAGTGATGTGCAAGAGTC	
Human	Forward	GGAGCACTGTGTTTATGCTGGAA	NM_003255
TIMP2	Reverse	GACCGAGCGATTGCTCAAGA	
Human	Forward	AGCGACTCGCCAGAGTGGTTA	NM_000660
TGFβ1	Reverse	GCAGTGTGTTATCCCTGCTGTCA	
Human	Forward	GCACCGTCAAGGCTGAGAAC	NM_002046
GAPDH	Reverse	TGGTGAAGACGCCAGTGGA	
Mouse	Forward	CCTGGCAAAGACGGACTCAAC	NM_007742
Col1A1	Reverse	GCTGAAGTCATAACCGCCACTG	
Mouse	Forward	TCCCTGGAGAAGAGCTACGAACT	NM_007392
αSMA	Reverse	AAGCGTTCGTTTCCAATGGT	
Mouse	Forward	TGCACCACCAACTGCTTAG	NM_008084
GAPDH	Reverse	GGATGCAGGGATGATGTTC	

Col1A1, α1 (I) collagen; GAPDH, glyceraldehyde 3-phosphate dehydrogenase; MMP, matrix metalloproteinase; αSMA, α-smooth muscle actin; TIMP, tissue inhibitor of matrix metalloproteinase.

Biosystems, Foster City, California, USA). As controls, normal liver tissues were taken from four patients who underwent resection for metastatic liver tumours.

Microarray analysis

In 22 of the 35 patients with chronic hepatitis C and in four controls, microarray analysis was performed using 10 μg total RNA with the 3D-Gene Human miRNA Oligo chip v10.1 (Toray, Tokyo, Japan), as described in detail elsewhere.[25]

Mouse model of liver fibrosis

Male C57BL/6 mice, 7–10 weeks old, were purchased from Japan SLC, Inc (Shizuoka, Japan). All animals received humane care. The experimental protocol was approved by the Committee of Laboratory Animals according to institutional guidelines. Mice (n=5) were injected intraperitoneally with 200 μg/g body weight of thioacetamide (TAA, Sigma) diluted in saline three times a week for 4 or 8 weeks.[26] Control mice (n=5) were injected with saline. As another liver fibrosis model, mice were given either a methionine- and choline-deficient diet (MCDD, n=7) or methionine-choline control diet (MCCD, n=7) for 5 or 15 weeks, as previously described.[27] In addition, a similar model was generated in rats by giving them MCCD for 10 weeks, MCDD for 10 weeks, or MCDD for 8 weeks followed by MCCD for the last 2 weeks (recovery group).[27] The ingredients for these diets were purchased from MP Biomedicals (Solon, Ohio, USA).

Cells

Primary stellate cells were isolated from male C57BL/6 mice by the pronase-collagenase digestion method[28] and were cultured in DMEM supplemented with 10% FBS. Hepatocytes were isolated by collagenase digestion. One day after culturing, the cells were treated with TGFα (1–10 ng/ml), TNFα (0.1–1 ng/ml), or QNZ (10–100 nmol/l) for 24 or 72 h. LX-2 (donated by Dr Scott Friedman[29]), NIH3T3 and Huh7 cells were maintained on plastic culture plates in DMEM supplemented with 10% FBS. HepG2 cells (JCRB1054), obtained from the Health Science Research Resources Bank (Osaka, Japan), were maintained on plastic culture plates in Minimum Essential Medium (Invitrogen, Carlsbad, California, USA) supplemented with 10% FBS, 1 mM sodium pyruvate (Invitrogen) and 1% non-essential amino acids (Invitrogen).

Quantitative real-time PCR

Total RNA was extracted from cells and liver tissues using the miRNeasy Mini Kit (Qiagen). cDNAs were synthesised using 0.5 μg of total RNA, a ReverTra Ace qPCR RT Kit (Toyobo, Osaka, Japan) and oligo(dT)$_{12-18}$ primers, according to the manufacturer's instructions. Gene expression was measured by real-time PCR using the cDNAs, THUNDERBIRD SYBR qPCR Mix Reagents (Toyobo) and gene-specific oligonucleotide primers (listed in table 2) with an ABI Prism 7500 Real-Time PCR System (Applied Biosystems). The GAPDH level was used to normalise the relative abundance of mRNAs. To detect miRNA expression, the RT reaction was performed using the TaqMan MicroRNA Assay (Applied Biosystems). Primers for PCR reactions in the miRNA assays were obtained from Applied Biosystems.

Immunoblotting

Proteins (20 μg) were subjected to sodium dodecyl sulphate–polyacrylamide gel electrophoresis and then transferred onto Immobilon P membranes. After blocking, the membranes were treated with primary antibodies followed by peroxidase-conjugated secondary antibodies. Immunoreactive bands were visualised by the enhanced chemiluminescence system using the Fujifilm Image Reader LAS-3000 (Fuji Medical Systems, Stamford, Connecticut, USA).

Transient transfection with miRNA precursors and inhibitors

Precursors or inhibitors of miR-222 and the negative control miRNA were transfected into human and mouse stellate cells using Lipofectamine RNAiMAX Transfection Reagent (Invitrogen) at a final concentration of 50 nmol/l, as previously described.[30 31] After 6 h, the culture medium was changed. Then, after 24 h, the cells were collected for total RNA and protein extraction.

Luciferase reporter assay

The interaction of the *CDKN1B* 3′UTR with miR-222 was assayed basically according to a previously described method.[30 31] The *CDKN1B* 3′UTR was obtained by PCR using human stellate cell cDNA as a template and the primer set forward 5′-TTCTCGAGGTTCTTGTCTTGATGTGTCACC-3′, reverse 5′-TTTCTAGAGAGAGCAGAGGCCTGAGAAG-3′. The Dual-Glo Luciferase Assay System (Promega, Madison, Wisconsin, USA) was used to analyse luciferase expression, according to the manufacturer's protocol.

Cell proliferation assay

LX-2 cells were plated at a density of 3×10^3 cells/well in 96-well plates for 24 h and were then transfected with the miR-222 precursor or inhibitor as described above. After 24 h, the medium was changed and culturing was continued for an additional

1–3 days before measuring cell proliferation by the WST-1 assay.[31]

Statistical analysis

Data, presented as box plots, are the median, IQR, minimum and maximum. The Mann–Whitney U test was used to analyse the distribution of continuous variables. The Jonckheere–Terpstra test for ordered alternatives was used to identify trends among classes. Correlation coefficients between parameters were evaluated by Spearman rank correlations. A two-tailed p value <0.05 was considered significant.

RESULTS

Patient characteristics

Table 1 shows the baseline characteristics of the patients infected with HCV and those with NASH who were included in this study. There were no significant differences in clinical, biochemical, haematological, virological, or histological characteristics between the 22 patients with HCV who were analysed by microarray and the 13 patients with HCV who were not.

miRNA expression profile in patients with HCV

We comprehensively compared miRNA expression profiles between cases of mild liver fibrosis (F1/F2) and advanced liver fibrosis (F3/F4) among the 22 patients with HCV using microarray analysis. As shown in the heat map in figure 1, 18 miRNAs were significantly upregulated (fold change, 1.21 to 2.59), whereas six miRNAs were significantly downregulated (fold change, −1.69 to −1.20) in livers with advanced fibrosis. Among the 18 overexpressed miRNAs, p values of <0.01 were found for miR-222 (fold change, 1.80), miR-214 (fold change, 1.84), miR-199a-3p (miR-199b-3p) (fold change, 1.90) and miR-199a-5p (fold change, 2.00). Among the six downregulated miRNAs, miR-422a (fold change, −1.69) showed a p value <0.01. Among them, the abundance of miR-199a-5p and miR-199a-3p has previously been reported to be increased in fibrotic liver disease.[32]

Next, we quantitatively confirmed our miRNA expression results in 35 patients with HCV (table 1) using real-time PCR. miR-199a-5p, miR-199a-3p and miR-222 were significantly upregulated in a stepwise manner according to the progression of liver fibrosis (figure 2A). miR-222 forms a cluster with miR-221 in the human and mouse genomes. In fact, miR-221 expression was significantly upregulated in patients with HCV with severe fibrosis (figure 2A). Col1A1 mRNA expression also significantly increased with increasing progression of liver fibrosis (figure 2B) and was significantly correlated with the expression of miR-222 (r=0.843, p<0.001) (figure 2C). Additionally, αSMA mRNA expression tended to increase according to the progression of fibrosis (figure 2B) and was significantly correlated with the expression of miR-222 (r=0.701, p<0.001) (figure 2C).

MicroRNA-221/222 expression in patients with NASH

We also validated miR-221 and miR-222 expression in 26 patients with biopsy-proven NASH (F1, seven; F2, eight; F3, eight; F4, three) by real-time PCR. The expression of these miRNAs was significantly upregulated in a manner dependent on the progression of liver fibrosis (figure 3A). Col1A1 mRNA expression was also significantly upregulated (figure 3B) and correlated with the expression of miR-222 (r=0.626, p<0.001) (figure 3C). In contrast, the expression level of αSMA mRNA tended towards a correlation with that of miR-222, but this result was not significant (r=0.375, p=0.059) (figure 3B,C). These results indicate the close correlation between miR-222 and Col1A1 mRNA expression in human liver fibrosis caused by NASH.

Expression of miR-221/222 in rodent models of liver fibrosis

Next, we studied miR-221 and miR-222 expression in mouse models of liver fibrosis. First, liver fibrosis was induced in mice by injecting TAA for 8 weeks. As shown in figure 4A, haematoxylin and eosin staining and Sirius red staining confirmed the occurrence of liver fibrosis, in particular around the central vein

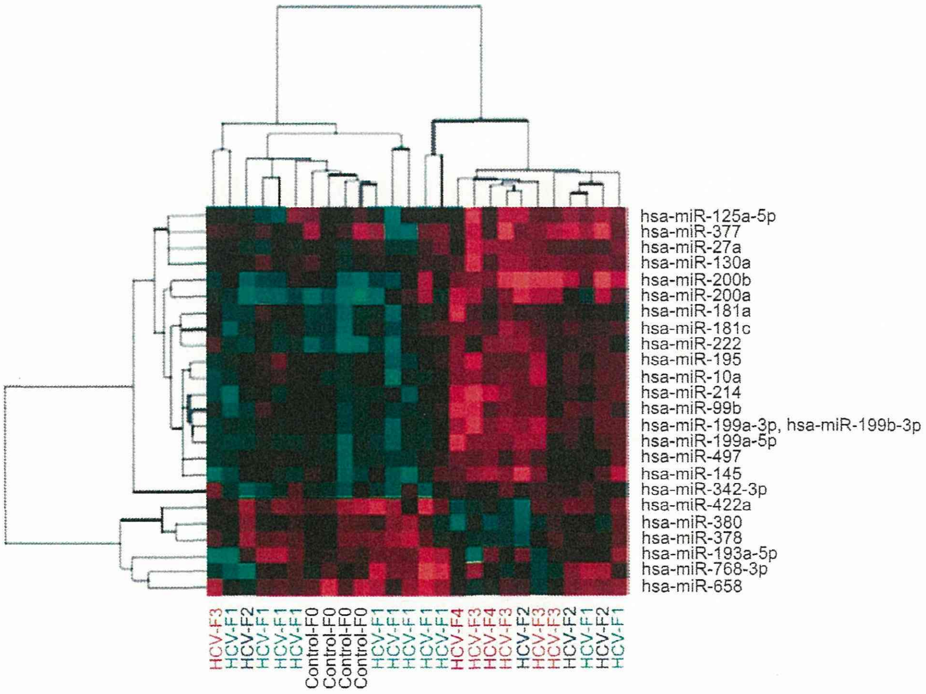

Figure 1 Heat map of microRNA (miRNA) expression in human liver tissue. Shown is the clustering of patients (n=22) with chronic hepatitis C by comprehensive analysis of intrahepatic miRNA expression according to the degree of hepatic fibrosis in biopsy specimens. Green and red denote downregulated and upregulated genes, respectively. F, fibrosis stage; HCV, hepatitis C virus.

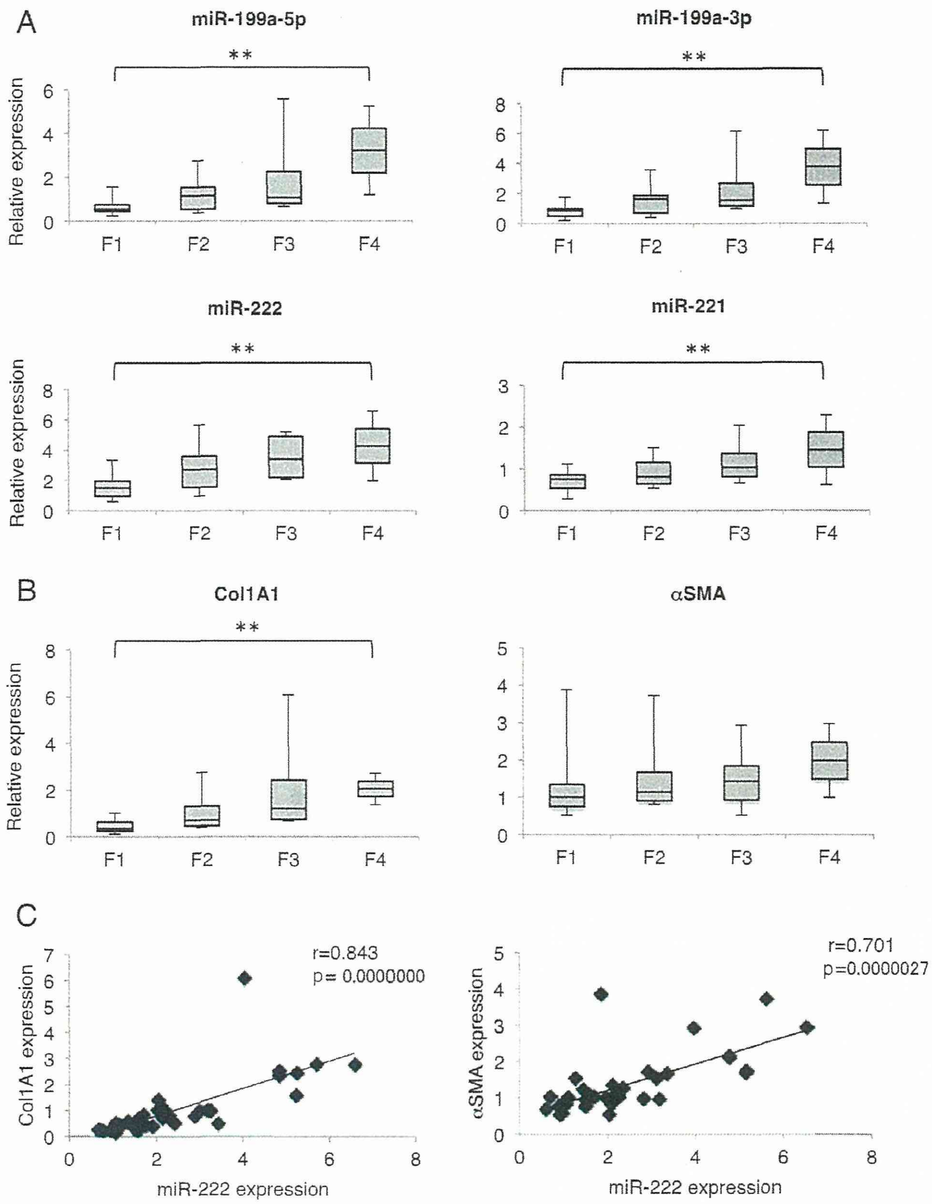

Figure 2 MicroRNA (miRNA) levels and their correlations with Col1A1 and α-smooth muscle actin (αSMA) mRNA expression in patients with chronic hepatitis C. (A) Expression of miR-199a-5p, miR-199a-3p, miR-222 and miR-221 in 35 patients with hepatitis C virus (HCV) with fibrosis. The expression levels are indicated relative to F1. The Jonckheere–Terpstra test for ordered alternatives was used to identify trends among classes. **$p<0.01$. (B) Expression of Col1A1 and αSMA mRNAs in 35 patients with HCV with fibrosis. The expression levels are indicated relative to F1. Glyceraldehyde 3-phosphate dehydrogenase was used as an internal control. The Jonckheere–Terpstra test for ordered alternatives was used to identify trends among classes. **$p<0.01$. (C) Correlation between miR-222 expression and Col1A1 or αSMA mRNA expression. Correlation coefficients between parameters were evaluated by Spearman rank correlations.

area. These mouse livers exhibited significant upregulation of the expression of Col1A1 (3.1-fold, $p<0.05$) and αSMA (1.9-fold, $p<0.05$) mRNAs compared with the control livers at 8 weeks (figure 4B). The expression of miR-221 and miR-222 increased by 1.8-fold ($p=0.06$) and 1.4-fold ($p<0.01$), respectively, at 8 weeks after TAA injection (figure 4C). The increased expression of miR-222 was accompanied by increased Col1A1 ($p<0.05$) and αSMA mRNA expression ($p<0.01$) (data not shown). Another liver fibrosis model was produced in mice by feeding them an MCDD. miR-221 and miR-222 increased by 2.4-fold ($p<0.01$) and 2.6-fold ($p<0.01$), respectively, in livers of mice fed MCDD for 15 weeks compared with those fed MCCD for 15 weeks (figure 4D). These results confirm that the increased expression of miR-221/222 in fibrotic livers is reproduced in mouse models. In addition, miR-221 and miR-222 expression increased in rats administered MCDD for 10 weeks, but returned to the level of the controls after 2 weeks on MCCD in the recovery group (figure 4E). These data clearly indicate the correlation between the increase in miR-221/222 and liver fibrosis.

Expression of miR-222 in hepatic stellate cells

According to the data obtained from human and rodent fibrotic livers, we assumed that stellate cells may contribute to the increases of miR-222 and its homologue miR-221. As expected, the expression of both miR-221 and miR-222 increased during the activation process of mouse stellate cells in primary culture (6.1- and 26.8-fold increases in miR-221 and 4.1- and 13.9-fold increases in miR-222 at day 4 and day 7 compared with day 1, respectively), in a manner similar to the mRNA expression of Col1A1 and αSMA (38.3- and 61.3-fold increases in Col1A1 mRNA and 6.1- and 6.9-fold increases in αSMA at day 4 and day 7 compared with day 1, respectively) (figure 5A,B). Isolated mouse hepatocytes expressed both miRNAs in smaller amounts than with the activated stellate cells (figure 5A). In addition, both miR-221 and miR-222 expression were significantly higher in LX-2 than in HepG2 cells (9.5- and 6.0-fold, respectively), Huh7 cells (9.2- and 4.4-fold, respectively) and NIH3T3 cells (1.1- and 3.2-fold, respectively) (figure 5C), confirming the relative specificity of the miRNA expression in activated stellate cells.